

## **CYCLIC DYNAMICS CAUSED BY ANTIGENIC DRIFT**

# CYCLIC DYNAMICS CAUSED BY ANTIGENIC DRIFT

By

RUI ZHANG, B.Eng. B.Sc.

A Project

Submitted to the School of Graduate Studies

in Partial Fulfilment of the Requirements

for the Degree

Master of Science

McMaster University

©Copyright by Rui Zhang, August 2005

MASTER OF SCIENCE (2005)  
(Mathematics)

McMaster University  
Hamilton, Ontario

TITLE: Cyclic dynamics caused by antigenic drift

AUTHOR: Rui Zhang  
B.Eng.  
Qingdao University, P.R.China  
B.Sc.  
McMaster University, Canada

SUPERVISORS: Dr. David J.D. Earn  
Dr. Junling Ma

NUMBER OF PAGES: vii, 53

*To my wife, Miao*

# Abstract

Traditionally, seasonal forcing has been considered to be the major cause of the influenza seasonality. However, Andreasen [2003] showed that repetitive introductions of new strains can lead to cyclic dynamics. The cyclic dynamic produced by his model is not seasonal, because the length of seasons cannot be defined in his model. In this report, we develop a model that combines a stochastic mutation process with a two-strain competition process governing the spread of the mutant strain. This model can produce stable seasonal dynamics. If we introduce a small seasonal forcing to the transmission rate, the length of a season can be regulated to one year if the unforced system oscillates with a period close to one year. If the system has a period that is far from one year, then the forced system may behave chaotically.

# Acknowledgments

I would like to thank Dr. David Earn and Dr. Junling Ma for their supervision of this project and for their patience. I would also like to thank to Dr.Gail Wolkowicz and Dr. Dmitry Pelinovsky for reading my report and providing constructive criticisms and insightful comments.

I am thankful to colleagues Dr. Daihai He, Dr. Lin Wang and Guihong Fan for the valuable discussions we had related to my project.

To my mom and dad, I am deeply indebted for their love and for giving my life. To my wife Miao, I am deeply thankful for her support during our time in Canada. I am also grateful to my sister and brother-in-law for taking care of dad on my behalf.

# Contents

|          |  |           |
|----------|--|-----------|
| <b>1</b> | <b>Introduction</b>  | <b>1</b>  |
| 1.1      | Biological background . . . . .                                    | 2         |
| 1.1.1    | The epidemiology of flu . . . . .                                  | 2         |
| 1.1.2    | Cross-immunity . . . . .   | 4         |
| 1.2      | Flu modeling . . . . .   | 4         |
| 1.2.1    | The SIR model . . . . .  | 4         |
| 1.2.2    | The SIRS model . . . . .   | 6         |
| 1.2.3    | The seasonally forced SIRS model . . . . .                         | 7         |
| 1.2.4    | The model of Andreasen [2003] . . . . .                            | 8         |
| 1.2.5    | The multi-strain competition model . . . . .                       | 9         |
| 1.2.6    | The individual-based model . . . . .                               | 10        |
| 1.3      | The organization of this report . . . . .                          | 11        |
| <b>2</b> | <b>The model</b>   | <b>12</b> |
| 2.1      | The mutation process . . . . .                                     | 13        |
| 2.1.1    | The first mutation time . . . . .                                  | 14        |
| 2.1.2    | The second mutation time . . . . .                                 | 16        |
| 2.2      | Infection history, cross-immunity and antigenic distance . . . . . | 17        |
| 2.3      | The mutant-parent competition . . . . .                            | 20        |

|          |  |           |
|----------|--|-----------|
| 2.4      | The combination of the mutation process and the competition process                      | 23        |
| 2.4.1    | A proper initial condition   | 24        |
| 2.4.2    | Reducing the dimension of the competition model (2.10)                                   | 26        |
| 2.4.3    | The sustained epidemics  | 26        |
| <b>3</b> | <b>The length of a season</b>  | <b>28</b> |
| 3.1      | The dependence on the basic reproduction number $\mathcal{R}_0$                          | 29        |
| 3.2      | The dependence on the mutation rate $\alpha$   | 29        |
| 3.3      | The dependence on the population size $N$  | 31        |
| 3.4      | The dependence on the cross-immunity parameters $\sigma_1$ and $\sigma_K$                | 32        |
| <b>4</b> | <b>Comparison to the model of Andreasen [2003]</b>                                       | <b>35</b> |
| 4.1      | Reducing the competition model Eqs. (2.10) to the model of Andreasen [2003]              | 35        |
| 4.2      | Differences between the dynamics of our model and those of the model of Andreasen [2003] | 36        |
| <b>5</b> | <b>Regulating the length of seasons</b>  | <b>40</b> |
| <b>6</b> | <b>Conclusions and discussions</b>   | <b>43</b> |

# Chapter 1

## Introduction

Influenza is a major cause of human morbidity and mortality all over the world. Flu epidemics sweep throughout the world and infect around 10% of the population every year [Monto, 2003]. In the United States and Canada alone, they kill thousands of people each year [Health Canada, 2003, Centers for Disease Control and Prevention, 2005]. The largest pandemic in the last century, the 1918 "Spanish flu", supposedly infected more than one third of the population of the United States [Holmes, 2004], and killed more than twenty million individuals worldwide [Kilbourne, 1987, Simonsen et al., 1998, Johnson and Mueller, 2002]. Two less severe pandemics, which occurred in 1957 and 1968, did not kill as many people as the 1918 flu, but caused major morbidity. After more than 400 years since an influenza epidemic was first described with reasonable certainty in 1557 [Nicholson et al., 1998], we are still far from controlling the disease.

In order to develop control strategies, we have to understand flu dynamics. Especially, we need to understand why the flu keeps coming back every year. Seasonality is the most striking characteristic of figure 1.1, which shows the monthly pneumonia and influenza deaths in United States from 1910 to 1998. In this project,

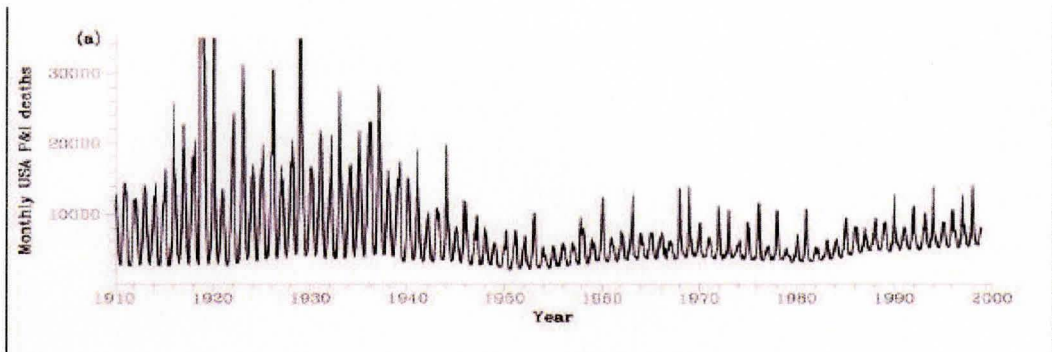


Figure 1.1: Monthly pneumonia and influenza (P&I) deaths from 1910 to 1998 in the United States. Copyright (2002), TRENDS in Ecology and Evolution [Earn et al., 2002]. The flu seasonality is a striking characteristic.

we try to develop a model that can explain its seasonality. Before we proceed to modeling, we will review the biological background.

## 1.1 Biological background

### 1.1.1 The epidemiology of flu

Three types of flu, A, B, and C, currently circulate in human populations. Flu A is further categorized into subtypes with notations of the form  $H_aN_b$ , where "a" describes the  $a$ -th found hemagglutinin (HA) protein and "b" describes the  $b$ -th found neuraminidase (NA) protein. Subtypes are further divided into strains and each genetically distinct virus is usually considered as a distinct strain [Earn et al., 2002].

Subtypes emerge from dramatic genetic changes (called antigenic shift), probably from genetic reassortments of different flu viruses within the host. In last century all three flu pandemics were caused by the introduction of a new subtype [Webster et al., 1992, Reid and Taubenberger, 2003]: the 1918 Spanish is caused by the introduction of  $H_1N_1$ , the 1957 Asian flu is caused by  $H_2N_2$ , the 1968 Hongkong flu is

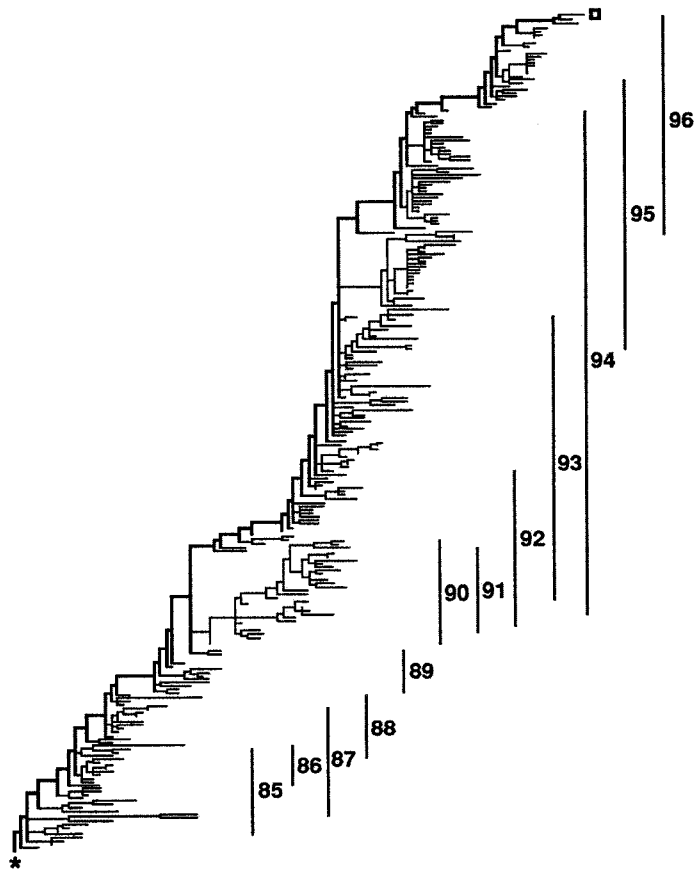


Figure 1.2: The phylogenetic tree of  $H_3N_2$  subtype of flu A in  $HA_1$  domain. Copyright (1997), National Academic of Science [Fitch et al., 1997]. Subtype  $H_3N_2$  mutates quickly.

caused by  $H_3N_2$  [Webster et al., 1992].

Flu A virus also undergoes fast mutations (called antigenic drift). Its mutation rate is probably only second to HIV [Fitch et al., 1997]. However, unlike HIV, the flu A phylogenetic tree (Figure 1.2) has a remarkable single trunk shape.

The basic reproduction number (the average number of secondary infections caused by an infectious individual in a totally susceptible population) is estimated to be  $\mathcal{R}_0 = 4 - 16$ ; the average infectious period is estimated to be  $T_{\text{inf}} = 4 - 8$  days

[Douglas, 1975, Fine, 1982, Pease, 1987].

### **1.1.2 Cross-immunity**

Evidence shows that when an individual is infected by a strain, he/she acquires not only life-time immunity to the specific strain, but some protection to similar strains as well [Nicholson et al., 1998]. This cross protection is called cross-immunity. However, because of the fast mutation of the flu virus, our immune system has to catch up with the virus, which, arguably, selects for faster mutation in some areas of the flu genome [Bush et al., 1999, Plotkin and Dushoff, 2003].

If the cross-immunity depends on the challenging strain, then it is called specific immunity. If it is the same for all possible challenging strains, then it is called nonspecific immunity.

## **1.2 Flu modeling**

In this section, we will review some common models applicable to the flu, and discuss their strengths and shortcomings.

### **1.2.1 The SIR model**

A major type of modeling in epidemiology is compartmental model. This approach divides the population into disjoint classes and follows the flow of individuals among the classes. In its simplest form, with the assumption that an individual will acquire life-time immunity after he/she recovers, the population can be divided into three classes: susceptible, infectious, and removed [Bailey, 1975, Anderson and May, 1991]. The individuals that have not been infected are in the susceptible class. Once they

are infected, they enter the infectious class and begin infecting others. After they recover, they enter the removed class and cannot be infected again (thus removed from the transmission process). This process can be illustrated by the following:



Let  $S$ ,  $I$ ,  $R$  be the proportions of the population in the susceptible, infectious and removed classes respectively. Assuming homogeneous mixing (each pair of individuals has the same probability of making a contact), a constant transmission rate  $\beta$ , and a recovery rate  $\gamma$ , we can write down a system of ordinary differential equations (ODEs) to describe the transmission process:

$$\dot{S} = -\beta SI, \tag{1.1a}$$

$$\dot{I} = \beta SI - \gamma I, \tag{1.1b}$$

$$\dot{R} = \gamma I. \tag{1.1c}$$

By adding up the equations, we see that  $S + I + R \equiv 1$  is invariant. The first octant is positively invariant because either the boundary planes are invariant ( $S = 0$  and  $I = 0$ ), or on the boundary ( $R = 0$ ), the trajectory points to the interior. Thus  $S$ ,  $I$ , and  $R$  are non-negative.

From Eq. (1.1b), when a disease is introduced into a completely susceptible population at time  $t = 0$ , *i.e.*,  $S(0) \approx 1$ ,  $I(t)$  can grow if and only if  $\mathcal{R}_0 = \frac{\beta}{\gamma} > 1$ . The threshold  $\mathcal{R}_0$  is the basic reproduction number of the model, which is defined as the mean number of secondary infections caused by an infectious individual in a completely susceptible population.

This model has an interesting property: the disease will eventually burn out,

i.e.,  $\lim_{t \rightarrow \infty} I(t) = 0$ . In fact, since  $\frac{d}{dt}(S+I) = -\gamma I$ ,  $V = S+I$  is a Lyapunov function of Eqs. (1.1) in the first octant. Thus the trajectories have to approach  $\dot{V} = 0$ , that is,  $I = 0$ .

Because of the life-time specific immunity, this model can be used to describe the spread of a flu strain in the population. However, because of the "burn-out" property, this model can only describe a single epidemic, and cannot explain the recurrent epidemics.

### 1.2.2 The SIRS model

In order to get a recurrent epidemic, we need to recruit susceptibles. The recruitment may come from either the population dynamics (birth/migration), or the epidemiological dynamics (loss of immunity). For the flu, since the birth/migration rates are small compared to the epidemiological parameters, the population dynamics can be ignored. Here we only discuss the effect of the loss of immunity. Even though humans probably have life-time specific immunity to each flu-strain, effective loss of immunity is possible because of the fast mutation of the flu virus. The dominant strain in next season is likely to be different from the current dominant strain.

The simplest way to model the loss of immunity is to assume a fixed loss rate  $\rho$ . When an individual loses immunity, he/she reenters the susceptible class. Model (1.1) can then be modified as:

$$\dot{S} = -\beta SI + \rho R, \tag{1.2a}$$

$$\dot{I} = \beta SI - \gamma I, \tag{1.2b}$$

$$\dot{R} = \gamma I - \rho R. \tag{1.2c}$$

We can check that  $(S = 1, I = 0, R = 0)$  is an equilibrium, which is called the disease free equilibrium (DFE). The disease can invade a completely susceptible population if and only if the DFE is unstable. The stability of the DFE is determined by the basic reproduction number  $\mathcal{R}_0 = \frac{\beta}{\gamma}$  [Diekmann and Heesterbeek, 2000].

When  $\mathcal{R}_0 > 1$ , there is a unique global asymptotically stable positive equilibrium  $(S^* = \frac{\gamma}{\beta}, I^* = \frac{\rho}{\beta} \frac{\beta - \gamma}{\rho + \gamma}, R^* = \frac{\gamma}{\beta} \frac{\beta - \gamma}{\rho + \gamma})$  [Diekmann and Heesterbeek, 2000]. Moreover, when  $\mathcal{R}_0 > 1$ , the eigenvalues associated with this equilibrium may have non-zero imaginary parts, in which case the equilibrium is approached by damped oscillations. However, instead of producing periodic dynamics as we observed in the flu, this model predicts that  $I(t)$  converges to a constant.

### 1.2.3 The seasonally forced SIRS model

A common practice to model a seasonal epidemic is to assume that the transmission rate  $\beta$  of the SIRS model (1.2) is seasonally forced, *i.e.*, is a periodic function of time  $\beta(t)$ . This assumption is reasonable for the flu because the survival probability of the flu virus might depend on environmental temperature and humidity [Schulman and Kilbourne, 1962].

Dushoff et al. [2004] showed that even a small amplitude ( $< 5\%$ ) of seasonal forcing is capable of producing large oscillations in flu incidence. This is because for flu-like parameters, when  $\mathcal{R}_0 > 1$ , the positive equilibrium is a spiral node, with an intrinsic damped oscillation period close to one year. This damped oscillation then resonates with the seasonal forcing and produces large oscillations.

However, the assumption of the SIRS models that the loss rate  $\rho$  is constant is difficult to justify for the flu: individuals lose immunity when facing a new strain. The introduction of new strains does not occur continuously. Instead, we should

expect that the loss of immunity occurs in pulses when new strains are introduced. Indeed, we can detect these pulses when fitting a SIRS model with a time-dependent loss rate to the death curves [Finkenstadt et al., 2004].

#### 1.2.4 The model of Andreasen [2003]

Andreasen [2003] constructed a model to study the effect of these discrete introductions of new strains. To simplify the model, Andreasen assumed that an individual's cross-immunity to a new strain depends only on the number of seasons that have passed since the individual was last infected, and that this cross-immunity vanishes after  $n$  seasons.

Let  $\sigma_i$ ,  $i = 1, \dots, n$  be the susceptibility reduction factors (where  $1 - \sigma_i$  is the cross-immunity),  $S_i^m$  be the fraction of the population in season  $m$  whose susceptibility factor is  $\sigma_i$ . Before a new strain is introduced,  $\sum_{i=1}^n S_i^m = 1$ . Let  $I^m$  be the fraction of infectious individuals in season  $m$ , and  $R^m$  be the fraction of recovered individuals in season  $m$ . New strains are introduced at the end of each season, *i.e.*, when  $I^m(t) \approx 0$ . The transmission process of each season is governed by the following SIR model:

$$\dot{S}_i^m = -\beta\sigma_i S_i^m I, \quad (1.3a)$$

$$\dot{I}^m = \sum_{i=1}^n \beta\sigma_i S_i^m I - \gamma I, \quad (1.3b)$$

$$\dot{R}^m = \gamma I, \quad (1.3c)$$

where for each season  $m$ ,  $t \in [0, \infty)$ , and  $m = 0, 1, 2, \dots$ .  $R^m(\infty)$  contains individuals that are infected in season  $m$  and recovered. For season  $m + 1$ , these individuals were

infected exactly one season ago. Thus

$$S_1^{m+1}(0) = R^m(\infty).$$

Similarly, we have

$$S_{i+1}^{m+1}(0) = S_i^m(\infty), \quad i = 1, 2, \dots, n-2,$$

$$S_n^{m+1} = S_n^m(\infty) + S_{n-1}^m(\infty).$$

Andreasen [2003] showed that depending on  $\beta$  and  $\sigma_i$ , the infection history structure  $\{S_i^m(0)\}_{i=1}^n$  may have dynamics ranging from a stable equilibrium to complex cyclical behaviors.

Thus, seasonal epidemics occur in this model simply because of the introduction of new strains. However, this model does not explain where the new strains come from. Furthermore, since new strains are introduced manually at time  $t = \infty$  in each season, the length of a season cannot be properly defined in this model.

### 1.2.5 The multi-strain competition model

New strains come from either mutation or migration. If we consider a closed population, then the only source of new strains is mutation. Mutation only occurs when there are infectious individuals. Thus mutants should be introduced during, instead of after, an epidemic. Hence, when a mutation occurs, the mutant strain will compete with the parent strain.

In general, to study the dynamics of  $n$  competing strains, one must keep in mind that an individual's immunity to a specific strain depends on the individual's infection history. Let  $H = \{1, \dots, n\}$  be the strain space;  $S_L$  be the proportion of the

susceptible individuals who have been infected only by all the strains in set  $L \subset H$ ;  $I_L^i$  be the proportion of the infectious individuals who come from class  $S_L$  (infectious with strain  $i$ ) and  $\sigma_L^i$  be the susceptibility reduction factor (where  $1 - \sigma_i$  is the cross-immunity) of individuals in  $S_L$  to strain  $i$ . Then the competition is governed by the dynamical system

$$\dot{S}_L = -\beta \sum_{i \in H \setminus L} \sigma_L^i S_L I_L^i + \sum_{j \in L} \gamma I_{L \setminus j}^j, \quad L \subset H, \quad (1.4a)$$

$$\dot{I}_L^i = \beta \sigma_L^i S_L I^i - \gamma I_L^i, \quad L \subset H, i \in H \setminus L. \quad (1.4b)$$

There are  $(n + 1)2^n$  equations in the system (1.4). Andreasen et al. [1997] gave a rough analysis. Lin et al. [1999] analyzed three-strain systems. With some assumptions on cross-immunity  $\sigma_L^i$ , Dawes and Gog [2002] analyzed some four-strain systems. When  $n$  is large, it is difficult to analyze the model in detail. In fact, when  $n$  is large, the number of equations is comparable to the population size, which implies that most of the compartments are nearly empty. Thus it is hard to justify the use of ODE systems, which assumes an infinite population size in each class [Earn et al., 2002].

### 1.2.6 The individual-based model

One way to get around the problem of a large number of equations in the multi-strain competition model is to use individual-based models, which are stochastic models that keep track of the epidemiological details of each individual.

In an effort to reproduce the flu-A-like phylogenetic tree, Ferguson et al. [2003] built an individual-based model. In their model, strains are characterized by a pseudo-genome consisting of  $B$  epitopes, each consisting of  $C$  codons (3 nucleotide bases).

The genetic sequences of all the infected strains (the infection history) of each individual is recorded to compute the specific cross-immunity, which is a function of the antigenic distance between the challenging strain and the individual's infection history. Each infectious individual produces mutants of the currently infected strain at a fixed rate. This model also contains complex spatial and temporal structures: 20 patches with out-of-phase seasonal forcing to the transmission rates, and within patch spatial structures. A short-lived nonspecific immunity is introduced as well, which is found to be crucial for reproducing a flu-A like phylogenetic tree. With this model, they reproduced not only the phylogenetic tree, but the seasonal patterns of the flu dynamics as well.

However, because of its stochastic nature and the overwhelming details, this model is mathematically intractable.

### **1.3 The organization of this report**

In the next chapter, we build a model that couples the mutation process of Ferguson et al. [2003] and a multi-strain competition model within each season to overcome the problem of manually introducing strains at the end of each season. In Chapter 3, we will discuss dependencies of the length of seasons on different parameters. We will compare the results of our model to the results of the model of Andreasen [2003] in Chapter 4. Then we will study the effect of seasonally forced transmission rates on our model in Chapter 5. In Chapter 6, we conclude our results, and discuss the strengths and limitations of our model, and possible future areas of research.

# Chapter 2

## The model

Recall that Andreasen [2003] showed that recurrent epidemics can arise from repetitive introductions of new strains. However, his model requires that the mutant be introduced at time  $t = \infty$  in each season. Moreover, his results depend on a specific assumption: the immunity of an individual to a challenging strain depends only on the number of seasons from the last infection of the individual to the season of the challenge. It is difficult to justify this assumption without a description of how new strains emerge.

In this chapter, we develop a mutation model that naturally gives rise to the cross-immunity of Andreasen [2003]. Then we couple this mutation model with a transmission model to describe the spread of the mutants.

Since the birth/death and migration rates are tiny compared to the epidemiological rate parameters, they can be neglected. Thus, in this model, we will consider a closed population without population dynamics. Hence, the population size is a constant.

## 2.1 The mutation process

We model the mutation process after the model of Ferguson et al. [2003], which is an individual-based stochastic process. We assume that each infectious individual produces mutants of his/her currently infected variant independently with a constant rate  $\alpha_{\text{ind}}$ ; furthermore, when a mutation occurs, the mutant takes over its parental variant within the host. Thus the mutation process of each infectious individual is a Poisson process with rate  $\alpha_{\text{ind}}$ . On the population level, the mutation process is the sum of the individual mutation processes. Thus, it is a nonhomogeneous Poisson process with rate

$$\lambda(t) = \alpha_{\text{ind}}NI(t), \quad (2.1)$$

where  $N$  is the population size, and  $I(t)$  is the proportion of infectious individuals at time  $t$ . Since the population dynamic is ignored,  $N$  is a constant. We let  $\alpha = \alpha_{\text{ind}}N$ , which is the mutation rate of the population, so Eq. (2.1) can be rewritten as

$$\lambda(t) = \alpha I(t). \quad (2.2)$$

The expected number of mutations  $\Lambda$  in a season is

$$\begin{aligned} \Lambda &= \int_{T_s}^{T_e} \lambda(t) dt \\ &= \alpha \int_{T_s}^{T_e} I(t) dt, \end{aligned}$$

where  $T_s$  and  $T_e$  represent the start time and the end time of the season. Ma and Earn [to appear] showed

$$\int_{T_s}^{T_e} I(t) dt = ZT_{\text{inf}},$$

where  $T_{\text{inf}}$  is the expected infectious period ( $T_{\text{inf}} = \gamma^{-1}$ ), and  $Z$  is the expected final size of the epidemic. Thus we have

$$\Lambda = \alpha T_{\text{inf}} Z. \quad (2.3)$$

If we know the expected number of mutations ( $\Lambda$ ) and the final size  $Z$ , we can then estimate the mutation rate  $\alpha$  (or  $\alpha_{\text{ind}}$ ) from Eq. (2.3).

### 2.1.1 The first mutation time

Since the mutation process is a nonhomogeneous Poisson process with rate  $\lambda(t)$ , the first mutation time is exponentially distributed with the probability density function (PDF)

$$p(t) = \lambda(t) e^{-\int_{T_s}^t \lambda(\tau) d\tau}. \quad (2.4)$$

However,

$$\begin{aligned} \int_{T_s}^{T_e} p(t) dt &= \int_{T_s}^{T_e} \lambda(t) e^{-\int_{T_s}^t \lambda(\tau) d\tau} dt, \\ &= 1 - e^{-\int_{T_s}^{T_e} \lambda(\tau) d\tau}, \\ &= 1 - e^{-\Lambda} < 1, \end{aligned}$$

so for any season there is always a probability  $e^{-\Lambda}$  that no mutation occurs. This presents a problem because if no mutation occurs in a season, the epidemic is governed by an SIR model without recruitment of susceptibles. As we discussed in section 1.2.1, the disease will eventually die out. When  $\Lambda \ll 1$ , the probability of mutation is small. To avoid this problem, we assume that mutations always occur as long as there is an

epidemic. Specifically, the PDF of the first mutation time becomes

$$p(t) = \frac{\lambda(t)}{1 - e^{-\Lambda}} e^{-\int_{T_s}^t \lambda(\tau) d\tau}. \quad (2.5)$$

The expected first mutation time  $T_{\text{mut}}$  is

$$T_{\text{mut}} = \int_{T_s}^{T_e} t \frac{\lambda(t)}{1 - e^{-\Lambda}} e^{-\int_{T_s}^t \lambda(\tau) d\tau} dt. \quad (2.6)$$

Note that if the dynamics of a specific variant  $v$  can be described by the simple SIR model (1.1), then we can compute the expected mutation time  $T_{\text{mut}}$  relative to the peak time  $T_p$  of the epidemic.  $\lambda(t)$  depends on  $I(t)$ , which is a function of  $\mathcal{R}_0$ ,  $\gamma$  and  $I(0)$ . Since new variants always emerge from mutations, we assume  $I(0) = 1/N$ . Then  $\frac{T_{\text{mut}}}{T_p}$  is a function of  $\alpha$  and  $\mathcal{R}_0$ . For any  $Z$  (which is a function of  $\mathcal{R}_0$  [Diekmann and Heesterbeek, 2000, Ma and Earn, to appear]) and  $\Lambda$ , we can compute  $\alpha_{\text{ind}}$  from Eq. (2.3). Fitch et al. [1997] estimated that for the human population ( $N = 6 \times 10^9$ ),  $\Lambda \approx 5.7$  mutations per year. Because of the definition of  $\alpha$ , this estimate relates  $\frac{T_{\text{mut}}}{T_p}$  as a function of  $\mathcal{R}_0$  and  $N$ . For each  $\mathcal{R}_0$  and  $N$ , we numerically computed the solution of the SIR model (1.1) with the initial conditions  $I(0) = 1/N$ ,  $S(0) = 1 - I(0)$ , and  $R(0) = 0$ . We can then find the maximum of  $I(t)$  and the corresponding peak time  $T_p$ , and substitute  $I(t)$  into Eq. (2.2) to compute  $\lambda(t)$ . We then substitute  $\lambda(t)$  into Eq. (2.6) and compute  $T_{\text{mut}}$ . Figure 2.1 shows contour plots of the resulting  $\frac{T_{\text{mut}}}{T_p}$  as a function of  $N$  and  $\mathcal{R}_0$ , from which we can see that for a reasonable  $\mathcal{R}_0$  ( $\mathcal{R}_0 > 1.5$ ),  $T_{\text{mut}}/T_p > 0.8$ . In fact, for a population size comparable to China ( $N \approx 1.3 \times 10^9$ ) and  $1.5 < \mathcal{R}_0 < 6$ , the expected first mutation time  $T_{\text{mut}}$  occurs around the peak of the epidemic.

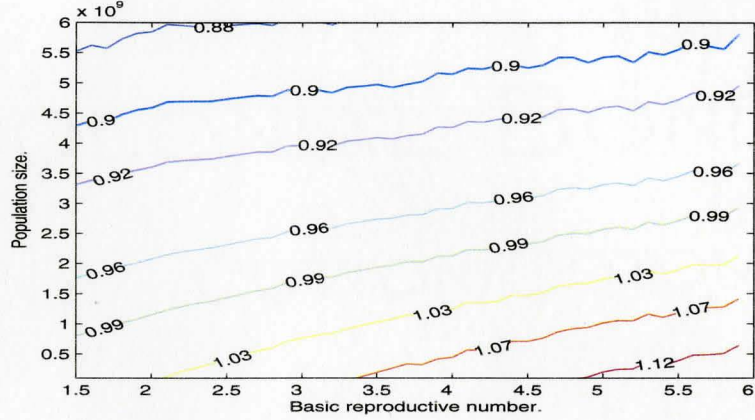


Figure 2.1: Contour plot of the relative mean first mutation time  $\frac{T'_{\text{mut}}}{T_p}$  vs. the population size  $N$  and the basic reproduction number  $\mathcal{R}_0$ . The first mutation occurs on average around the peak of an epidemic.

### 2.1.2 The second mutation time

Similarly, we can compute the expected time of second mutation, given that there is at least one mutation. Let the random variables  $T_1$  and  $T_2$  be the first and the second mutation time. We have

$$\begin{aligned} T'_{\text{mut}} &= E_{T_1} E [T_2 | T_1] \\ &= \int_{T_s}^{T_e} p(T_1) \int_{T_1}^{T_e} t \lambda(t) e^{-\int_{T_1}^t \lambda(\tau) d\tau} dt dT_1. \end{aligned}$$

As with the expected first mutation time  $T_{\text{mut}}$ ,  $\frac{T'_{\text{mut}}}{T_p}$  is a function of  $N$  and  $\mathcal{R}_0$ . This function is plotted in figure 2.2. We can see for a population size smaller or equal to that of China ( $N < 1.3 \times 10^9$ ), the second mutation occurs very late. Thus the first mutation will always dominate. Hence, for a population size comparable to or smaller than that of China, we can safely assume that each circulating variant produces at most one mutant.

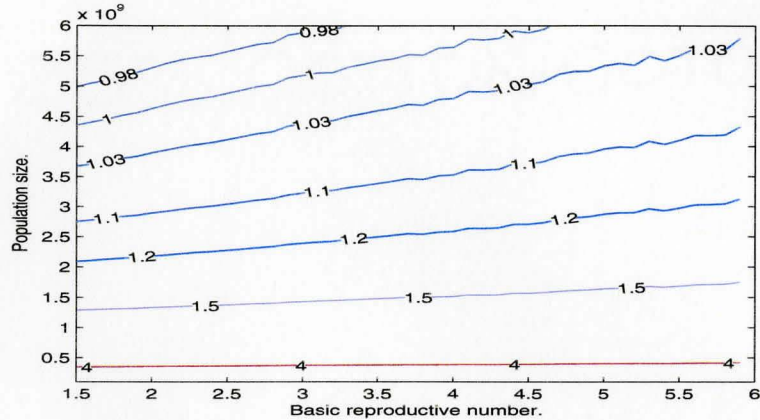


Figure 2.2: Contour plot of  $\frac{T'_{mut}}{T_p}$  vs. the population size  $N$  and the basic reproduction number  $\mathcal{R}_0$ , given that the first mutation occurs. We can see that the second mutation occurs late in the epidemic.

## 2.2 Infection history, cross-immunity and antigenic distance

The susceptibility of an individual to a new variant  $v$  generally depends on what variants he/she has ever been infected with previously (his/her infection history). In our model, we consider only specific immunity. We adapt the specific cross-immunity model introduced by Ferguson et al. [2003]: an individual's immunity to a new variant is a function of the antigenic distance of this variant and the set of previously infected variants in the antigenic space. We now define this antigenic distance precisely.

In order to define the antigenic distance, we need to describe the antigenic space. Suppose the immune system responds to  $P$  epitopes,  $P \gg 1$ , each containing  $M$  amino acids. Let  $\mathcal{E}$  be the space of all possible epitopes; since there are twenty different amino acids,  $\mathcal{E} = \{1, \dots, 20^M\}$ . In this project, we only study antigenic drift. We thus assume that each mutation changes a single amino acid out of  $PM$  possible ones, which in turn changes a single epitope. Then each variant  $v$  can be

characterized by a unique vector in the space  $\mathcal{S} = \mathcal{E}^P$ .

The antigenic distance  $d$  of two variants is defined by using the Hamming distance of two vectors, that is, the number of non-identical corresponding components of the two vectors. We denote  $v^i$  to be the  $i$ th component of variant  $v$ . Specifically, for two variants  $v_1$  and  $v_2$ , let

$$d_i(v_1, v_2) = \begin{cases} 1, & v_1^i \neq v_2^i, \\ 0, & v_1^i = v_2^i. \end{cases}$$

Then the antigenic distance of  $v_1$  and  $v_2$  is defined as

$$d(v_1, v_2) = \sum_{i=1}^P d_i(v_1, v_2).$$

The antigenic distance of a variant  $v$  and a set of variants  $H$  is defined as the number of components of  $v$  that do not appear at the corresponding position of any variant in  $H$ . Specifically, let

$$d_i(v, H) = \begin{cases} 0, & \prod_{u \in H} d_i(v, u) = 0, \\ 1, & \prod_{u \in H} d_i(v, u) \neq 0, \end{cases}$$

then

$$d(v, H) = \sum_{i=1}^P d_i(v, H).$$

Let  $v_n$  be the variant in the  $n$ th season. Because of the linear-phylogeny assumption,  $v_{n+1}$  is a mutant of  $v_n$ . Thus.

$$d(v_{n+1}, v_n) = 1.$$

Since we assumed that  $P \gg 1$ , it is unlikely for an epitope to mutate more than once.

Thus, we have

$$d(v_i, v_j) = |j - i|. \quad (2.7)$$

That is, with the linear-phylogeny assumption, the distance between two variants is the difference in their generations. In addition, if  $i_1 < i_2 < \dots < i_m < n$ , we have

$$d(v_n, \{v_{i_1}, v_{i_2}, \dots, v_{i_m}\}) = d(v_n, v_{i_m}) = n - i_m. \quad (2.8)$$

Eq. (2.8) ensures that the the antigenic distance of a challenging variant and an individual's infection history is the antigenic distance of the challenging variant and the individual's last-infected variant. Hence, the infection history can be characterized by the last-infected variant.

Thus the linear-phylogeny assumption leads to the infection history and cross-immunity used by Andreasen [2003].

Let  $\sigma_k$  be the susceptibility factor (where  $1 - \sigma_k$  is the cross-immunity) when the antigenic distance between the challenging variant and the infection history is  $k$ . We also assume that individuals have life-time immunity for all infected variants, *i.e.*  $\sigma_0 = 0$ . For a totally susceptible population, we denote the reduction as  $\sigma_\infty$ . Since totally susceptible individuals do not have any immunity,  $\sigma_\infty = 1$ .

Similarly to the model of Andreasen [2003], we assume that specific immunity diminishes when the challenging variant and the infection history is sufficiently different, *i.e.* there is a  $K$  such that  $\sigma_k = \sigma_K$  for  $k \geq K$ . This limit  $\sigma_K$  can be considered as the nonspecific immunity. Following Ferguson *et al.*, we pick  $\sigma_k$  to be

piecewise-linear:

$$\sigma_k = \begin{cases} \sigma_1, & k = 1, 2, \\ \sigma_K, & k \geq K, \\ \sigma_1 + \frac{\sigma_K - \sigma_1}{K-2}(k-2), & 2 < k < K, \\ 0, & k = 0, \\ 1, & k = \infty. \end{cases} \quad (2.9)$$

with two parameters  $0 < \sigma_1 < \sigma_K < 1$ .

## 2.3 The mutant-parent competition

Since mutants are introduced in the middle of each season, they face the competition of their parental variants. Recall that the first mutation is expected to occur around the peak of an epidemic. When a variant  $v_{n+1}$  is produced by  $v_n$ , the epidemic caused by  $v_{n-1}$  is usually finished. Thus we can assume that each mutant faces only the competition of its parental variant. In this section, we set up a two-strain competition model to describe the spread of the mutant. The model can be described by the flow chart shown in figure 2.3.

We denote by  $S_i$  the proportion of the individuals who have been infected by variant  $v_i$  but not by variants  $v_j$  for all  $j > i$ ,  $i = 0, 1, \dots, n-1$ , ( $S_0$  denotes the totally susceptible population). These individuals who are susceptible to variants  $v_j$  for all  $j > i$ , when infected by the variant  $v_n$  or its mutant  $v_{n+1}$ , enter the classes  $I_n$  and  $I_{n+1}$ , respectively, then recover and enter the classes  $S_n$  and  $S_{n+1}$ , respectively. The individuals in  $S_n$  and  $S_{n+1}$  can then be infected by  $v_{n+1}$  and  $v_n$ , and enter classes  $I_{n,n+1}$  and  $I_{n+1,n}$ . The individuals in classes  $I_{n,n+1}$  and  $I_{n+1,n}$  are infected (sequentially) by both  $v_n$  and  $v_{n+1}$  during the same season; they then recover and

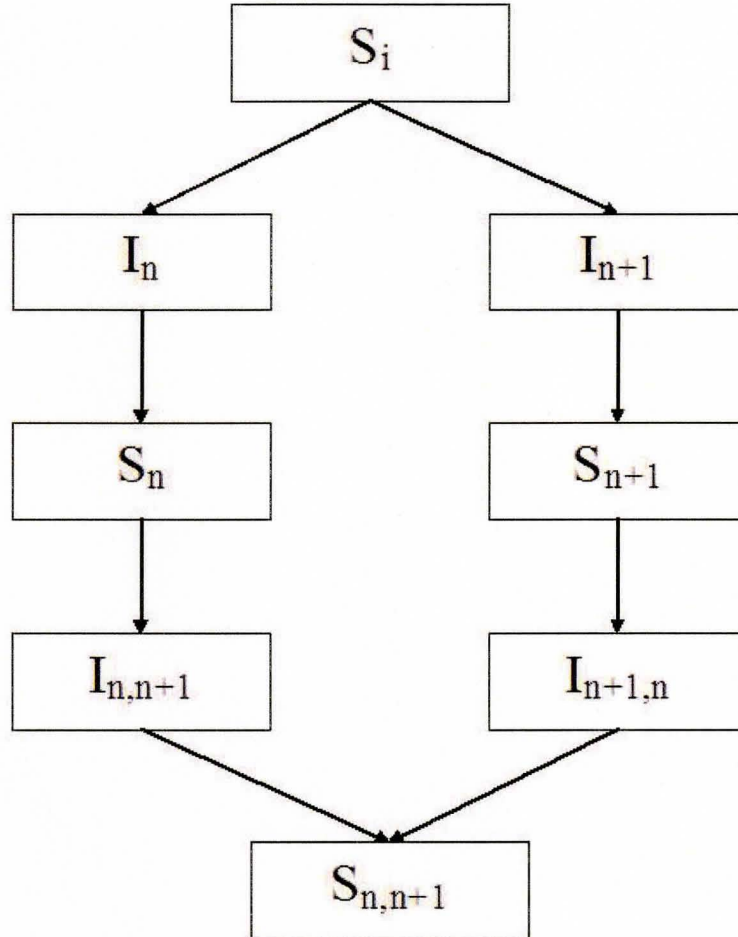


Figure 2.3: The flow chart of the two-strain competition model (Eqs. (2.10)), where  $S_i$ ,  $i \leq n$  are the proportions of individuals who have been infected by  $v_i$  but not  $v_k$  for  $k > i$ ;  $I_n$  and  $I_{n+1}$  are the proportion of individuals who come from  $S_i$  for  $i < n$  and is infectious with  $v_n$  and  $v_{n+1}$ , respectively;  $S_{n+1}$  are the proportion of individuals who have been infected by  $v_{n+1}$  but not  $v_n$ ;  $I_{n,n+1}$  and  $I_{n+1,n}$  are the proportion of individuals who come from  $S_n$  and  $S_{n+1}$ , respectively, and are infectious with  $v_{n+1}$  and  $v_n$ , respectively;  $S_{n,n+1}$  are the proportion of individuals who has been infected sequentially by  $v_n$  and  $v_{n+1}$  in the same season.

enter the class  $S_{n,n+1}$ . Moreover, we ignore cross infection, *i.e.*,  $I_i$  cannot infect  $I_j$  for all  $i$  and  $j$ . After the mutant  $v_{n+1}$  is introduced, the epidemic process is governed by the following system

$$\dot{S}_i = -\beta S_i [\sigma_{n-i}(I_n + I_{n+1,n}) + \sigma_{n+1-i}(I_{n+1} + I_{n,n+1})], \quad i < n, \quad (2.10a)$$

$$\dot{I}_n = \beta \sum_{i=1}^{n-1} \sigma_{n-i} S_i (I_n + I_{n+1,n}) - \gamma I_n, \quad (2.10b)$$

$$\dot{I}_{n+1} = \beta \sum_{i=1}^{n-1} \sigma_{n+1-i} S_i (I_{n+1} + I_{n,n+1}) - \gamma I_{n+1}, \quad (2.10c)$$

$$\dot{S}_n = -\beta \sigma_1 S_n (I_{n+1} + I_{n,n+1}) + \gamma I_n, \quad (2.10d)$$

$$\dot{S}_{n+1} = -\beta \sigma_1 S_{n+1} (I_n + I_{n+1,n}) + \gamma I_{n+1}, \quad (2.10e)$$

$$\dot{I}_{n,n+1} = \beta \sigma_1 S_n (I_{n+1} + I_{n,n+1}) - \gamma I_{n,n+1}, \quad (2.10f)$$

$$\dot{I}_{n+1,n} = \beta \sigma_1 S_{n+1} (I_n + I_{n+1,n}) - \gamma I_{n+1,n}, \quad (2.10g)$$

$$\dot{S}_{n,n+1} = \gamma (I_{n,n+1} + I_{n+1,n}), \quad (2.10h)$$

where  $n \geq 1$ ,  $t \geq T_{\text{mut}}^{n+1}$ , and  $T_{\text{mut}}^{n+1}$  is the creation-time of the variant  $v_{n+1}$ . We assume that only one individual is infected by the mutant  $v_{n+1}$  at the time of mutation, *i.e.*,  $I_{n+1}(T_{\text{mut}}^{n+1}) = \frac{1}{N}$  where  $N$  is the population size. At time  $T_{\text{mut}}^{n+1}$ , no infection of  $v_{n+1}$  has ever occurred, and thus  $S_{n+1}(T_{\text{mut}}^{n+1}) = S_{n,n+1}(T_{\text{mut}}^{n+1}) = I_{n,n+1}(T_{\text{mut}}^{n+1}) = I_{n+1,n}(T_{\text{mut}}^{n+1}) = 0$ .

Note that  $S_n(\infty)$  is the proportion of individuals who have been infected by  $v_n$  but not  $v_{n+1}$ , and  $S_{n+1}(\infty) + S_{n,n+1}(\infty)$  is the proportion of individuals who have been infected by  $v_{n+1}$ .

Throughout this report, we assume  $\gamma = 0.25/\text{day}$  (the mean infectious period is 4 days [Ferguson et al., 2003]). Thus the basic reproduction number  $\mathcal{R}_0 = 4\beta$  (where  $\beta$  is expressed in units of 1/day).

If  $\sigma_1 \ll 1$ , then  $I_{n,n+1}$  and  $I_{n+1,n}$  can be neglected. In this case, Eqs. (2.10) can be simplified to

$$\dot{S}_i = -\beta S_i(\sigma_{n-i}I_n + \sigma_{n+1-i}I_{n+1}), \quad i < n, \quad (2.11a)$$

$$\dot{I}_n = \beta \sum_{i=1}^{n-1} \sigma_{n-i} S_i I_n - \gamma I_n, \quad (2.11b)$$

$$\dot{I}_{n+1} = \beta \sum_{i=1}^{n-1} \sigma_{n+1-i} S_i I_{n+1} - \gamma I_{n+1}, \quad (2.11c)$$

$$\dot{S}_n = \gamma I_n, \quad (2.11d)$$

$$\dot{S}_{n+1} = \gamma I_{n+1}. \quad (2.11e)$$

## 2.4 The combination of the mutation process and the competition process

We have modeled the mutation process and the competition process. But these two processes are not independent: the mutation time  $T_{\text{mut}}^{n+1}$ , which is the initial time of the competition process (2.10), depends on the epidemic curve  $\tilde{I}_n(t) = I_n(t) + I_{n+1,n}(t)$  of the variant  $v_n$ , which in turn, depends on the mutation time  $T_{\text{mut}}^n$ . In this section, we combine the mutation process and the competition process into an iteration model.

Since  $T_{\text{mut}}^{n+1}$  depends on the epidemic curve  $\tilde{I}_n(t)$ , we need to substitute  $\tilde{I}_n(t)$  into Eq. (2.4) to generate a random mutation time, or, into Eq. (2.6) to compute the expected mutation time, where  $T_s = T_{\text{mut}}^n$  and  $T_e = \infty$ . In the rest of this report, we will use the expected mutation time unless specified. This makes our model deterministic.

Now that we can compute the mutation time  $T_{\text{mut}}^{n+1}$  of  $v_{n+1}$ , provided that we know the initial condition  $S_i(T_{\text{mut}}^{n+1})$ ,  $i \leq n$  and  $I_n(T_{\text{mut}}^{n+1})$ , we can then solve for the

competition model (2.10), and get the epidemic curve  $\tilde{I}_{n+1}(t)$  of the mutant  $v_{n+1}$ . We can thus repeat this process and find the mutation time  $T_{\text{mut}}^{n+2}$  of  $v_{n+1}$  and the epidemic curve  $\tilde{I}_{n+2}(t)$ , and keep doing so for all variants  $v_k$ ,  $k > n + 1$ .

Thus, we can solve for any epidemic provided we know the initial condition for the very first epidemic,  $S_0(0)$ , and  $I_1(0)$ .

### 2.4.1 A proper initial condition

The first epidemic starts when the ancestor variant  $v_1$  is introduced into a totally susceptible population. Thus,  $I_1(0) = \frac{1}{N}$ , and  $S_0(0) = 1 - \frac{1}{N}$ . The first epidemic is then governed by the simple SIR model (1.1). Note that from figure 2.1, when  $N$  is small,  $T_{\text{mut}}^2/T_p \approx 1$ . Thus  $\frac{\dot{I}_2(T_{\text{mut}}^2)}{I_2(T_{\text{mut}}^2)} = \beta S_0(T_{\text{mut}}^2) - \gamma \approx \beta S_0(T_p) - \gamma = 0$ . In fact, if  $T_{\text{mut}}^2 > T_p$ ,  $S_0(T_{\text{mut}}^2) < S_0(T_p)$ , thus  $\dot{I}_2(T_{\text{mut}}^2) < 0$ . That is, it is difficult or impossible to for the mutant  $v_2$  to invade. Thus when the mutant  $v_3$  of  $v_2$  invades,  $S_1(T_{\text{mut}}^3) = \int_{T_{\text{mut}}^2}^{T_{\text{mut}}^3} I_1(t) dt \approx 0$ ,  $S_1(T_{\text{mut}}^3) \approx S_1(T_{\text{mut}}^2)$  and  $S_2(T_{\text{mut}}^3) = \int_{T_{\text{mut}}^2}^{T_{\text{mut}}^3} I_2(t) dt \approx 0$ . Then

$$\dot{I}_3(T_{\text{mut}}^3) \approx \beta[S_0(T_{\text{mut}}^3) + \sigma_1(1 - S_0(T_{\text{mut}}^3))]I_3(T_{\text{mut}}^3) - \gamma I_3(T_{\text{mut}}^3).$$

Hence, we need  $S_0(T_{\text{mut}}^3) + \sigma_1(1 - S_0(T_{\text{mut}}^3)) > \frac{1}{\mathcal{R}_0}$  in order for  $v_3$  to invade, which is equivalent to

$$\sigma_1 > \frac{\frac{1}{\mathcal{R}_0} - S_0(T_{\text{mut}}^3)}{1 - S_0(T_{\text{mut}}^3)}. \quad (2.12)$$

From the solution  $Z$  of the final size formula of the SIR model [Diekmann and Heesterbeek, 2000]

$$1 - Z = e^{-\mathcal{R}_0 Z},$$

we can compute  $S_0(T_{\text{mut}}^3) = 1 - Z$ . In fact, the right hand side of Eq. (2.12) is a decreasing function of  $\mathcal{R}_0$ , thus the cross-immunity  $(1 - \sigma_1)$  increases with  $\mathcal{R}_0$  (figure

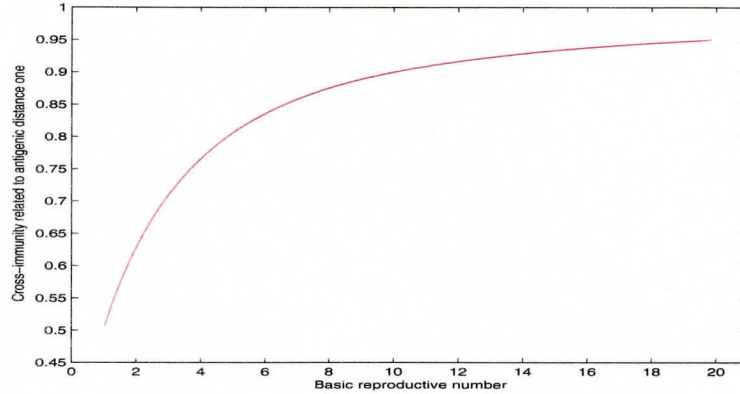


Figure 2.4: The maximum cross-immunity  $1 - \sigma_1$  for the invasion of the variant  $v_3$  vs. the reproduction number  $\mathcal{R}_0$ . Thus the cross-immunity  $1 - \sigma_1$  has to be very small in order for the disease to persist in a totally susceptible population.

2.4). Clearly, in order for  $v_3$  to invade, we need  $\sigma_1 \gg 0$ . Thus for a reasonable choice of parameters, the model cannot produce a sustained epidemic starting from a totally susceptible population. Indeed, this is a puzzle not only for our model (and the model of Andreasen [2003]), but also for explaining how real influenza epidemic survives after an antigenic shift [Earn et al., submitted].

Thus, we need to specify proper initial conditions  $S_i(T_{\text{mut}}^n)$ ,  $i < n$  and  $I_n(T_{\text{mut}}^n)$ . Unless specified, we set up the initial conditions  $S_i(T_{\text{mut}}^n)$ ,  $i < n$  and  $I_n(T_{\text{mut}}^n)$  using the following process: first, using the model of Andreasen [2003] (Eqs. (1.3)), we obtain a stable distribution of  $S_i^*$ ,  $i < n$ . We then set the initial conditions  $S_i(0) = S_i^*$  and  $I_n(0) = \frac{1}{N}$ , and let  $I_n(t)$  be the first epidemic. This enables us to compute an epidemic curve  $I_n(t)$ , which in turn, gives us the mutation time  $T_{\text{mut}}^{n+1}$ . We then use the values  $S_i(T_{\text{mut}}^{n+1})$  and  $I_n(T_{\text{mut}}^{n+1})$  as the initial condition for iteration.

### 2.4.2 Reducing the dimension of the competition model (2.10)

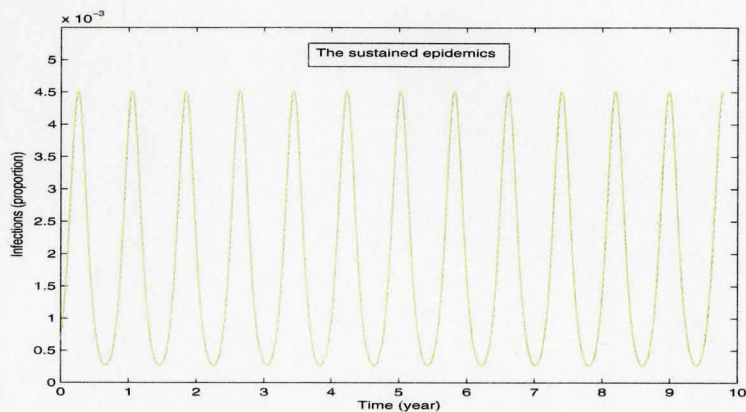
Now that we have an initial condition, the model is properly defined. However, as we iterate the model, the number for equations of the competition model (2.10) keeps growing with  $n$ . This presents both an analytical and a numerical challenge. In this section, we reduce the number of classes  $S_i$  in Eqs. (2.10).

Note that for each  $i$ ,  $\dot{S}_i(t) < 0$  for all  $t > T_{\text{mut}}^{i+1}$ , *i.e.*  $S_i(t)$  is a decreasing function. In fact, this is true as long as the disease does not die out, *i.e.*  $\limsup_{t \rightarrow \infty} \sum_{i=1}^{\infty} I_i(t) > 0$ ,  $S_i(\infty) = 0$  for all  $i$ . This is because  $\log S(\infty) = \log S(0) - \beta \sum_{i=1}^{\infty} \int_0^{\infty} I_i(t) dt = -\infty$ . Specifically, when  $n \gg 1$ , we can neglect  $S_0(t)$ . Since  $\sigma_k = \sigma_K$  for all  $k > K$ , the classes  $\{S_i\}_{i=1}^{n-K+1}$  can be combined into a single class  $S_K = \sum_{i=1}^{n-K+1} S_i$ .

### 2.4.3 The sustained epidemics

Figure 2.5 shows the total proportion of the population that is infectious,  $I(t) = \sum_{i=1}^{\infty} I_i(t) + I_{i+1,i}(t) + I_{i+1}(t) + I_{i,i+1}(t)$ , given by the solution to both our deterministic model and the stochastic model (where mutation time is generated randomly) with the following parameters:  $K = 12$ ,  $\sigma_1 = 0.01$ ,  $\sigma_K = 0.75$  as in the model of Ferguson et al. [2003],  $\mathcal{R}_0 = 5$ ,  $N = 6 \times 10^6$ , and  $\alpha_{\text{ind}} = 1.78 \times 10^{-9}$ . This figure shows that our model can produce sustained cyclic epidemics.

a)



b)

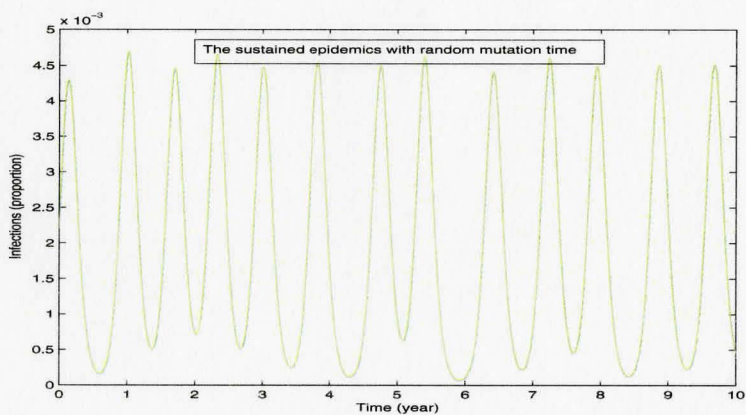


Figure 2.5: a) The epidemic curve  $I(t) = \sum_{i=1}^{\infty} I_i(t) + I_{i+1,i}(t) + I_{i+1}(t) + I_{i,i+1}(t)$  of our deterministic model with parameters  $K = 12$ ,  $\sigma_1 = 0.01$ ,  $\sigma_K = 0.75$ ,  $\mathcal{R}_0 = 5$ ,  $N = 6 \times 10^6$ ,  $\alpha_{\text{ind}} = 1.78 \times 10^{-9}$ . b) The epidemic curve  $I(t)$  of our stochastic model where the mutation time is generated randomly. This shows that our model can indeed produce stable periodic dynamics.

# Chapter 3

## The length of a season

For the cyclic epidemics produced by the deterministic model, we can define the start of a season as the time when the number of infectious individuals of the mutant variant equals that of its parent variant (figure 3.1), *i.e.*, the start time  $T_{\text{start}}^{n+1}$  of the season  $n + 1$  is the solution to the equation

$$I_n(t) + I_{n+1,n}(t) = I_{n+1}(t) + I_{n,n+1}(t). \quad (3.1)$$

The length of the  $n$ -th season  $L_n$  (also called the period) is then defined as  $L_n = T_{\text{start}}^{n+1} - T_{\text{start}}^n$ .

Note that when  $\sigma_1 \ll 1$ ,  $I_{n,n+1}(t)$  and  $I_{n+1,n}(t)$  can be neglected. Moreover, the mutant  $v_{n+1}$  is introduced around the peak of  $I_n(t)$ .  $I_n(t)$  monotonically decreases after the peak, while  $I_{n+1}(t)$  monotonically increases before the introduction of  $v_{n+2}$ . At the introduction of  $v_{n+2}$ ,  $I_n(t) \approx 0$ . Thus there is a unique solution to Eq. (3.1). Hence, the start time  $T_{\text{start}}^{n+1}$  is well defined.

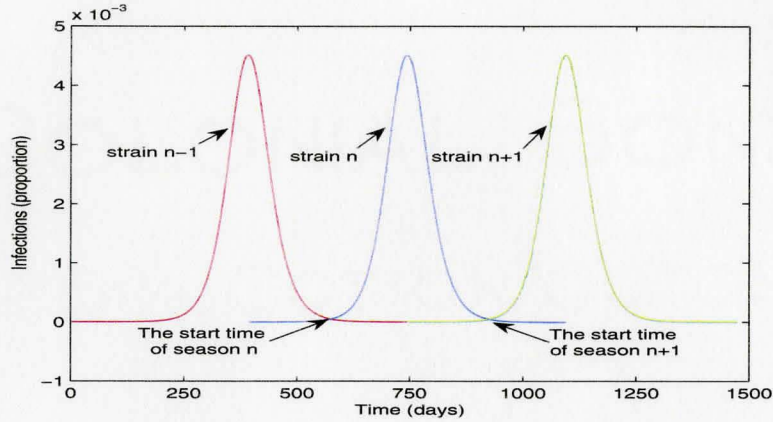


Figure 3.1: The definition of the start time of a new season  $T_{\text{start}}^n$ .

### 3.1 The dependence on the basic reproduction number $\mathcal{R}_0$

In this section we will keep the mutation rate  $\alpha_{\text{ind}}$ , the population size  $N$  and the cross-immunity parameters  $(1 - \sigma_1)$  and  $(1 - \sigma_K)$  fixed, and study the dependence of the length of season  $L_n$  on the basic reproduction number  $\mathcal{R}_0$ . Figure 3.2 shows the asymptotic trajectory (as  $n$  becomes large) of  $L_n$  versus  $\mathcal{R}_0$ , with parameters  $N = 6 \times 10^7$ ,  $\Lambda = 5.7$  (based on the population size of  $6 \times 10^9$ ),  $K = 12$ ,  $\sigma_1 = 0.01$ ,  $\sigma_K = 0.75$ . We can see that when  $\mathcal{R}_0 < 19$ ,  $L_n$  converges to a stable equilibrium, which decreases with  $\mathcal{R}_0$ ; when  $\mathcal{R}_0 > 19$ ,  $L_n$  bifurcates and eventually becomes chaotic (Fig. 3.3).

### 3.2 The dependence on the mutation rate $\alpha$

Now we keep  $\mathcal{R}_0$ ,  $N$ ,  $\sigma_1$  and  $\sigma_K$  constant and study how  $L_n$  varies with the mutation rate  $\alpha$ . The results are shown in figure 3.4, with parameters  $N = 1.3 \times 10^9$ ,  $\mathcal{R}_0 = 5$ ,

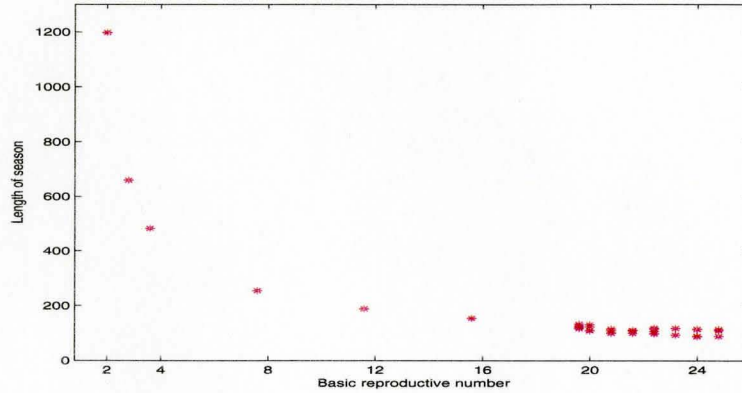


Figure 3.2: The asymptotic trajectory of season length  $L_n$  v.s.  $\mathcal{R}_0$ . This shows that the asymptotic season length generally decreases with the basic reproduction number  $\mathcal{R}_0$ . There is a bifurcation when  $\mathcal{R}_0 \approx 19$ . The parameters are  $N = 6 \times 10^7$ ,  $\Lambda = 0.057$ ,  $K = 12$ ,  $\sigma_1 = 0.01$ ,  $\sigma_K = 0.75$ .

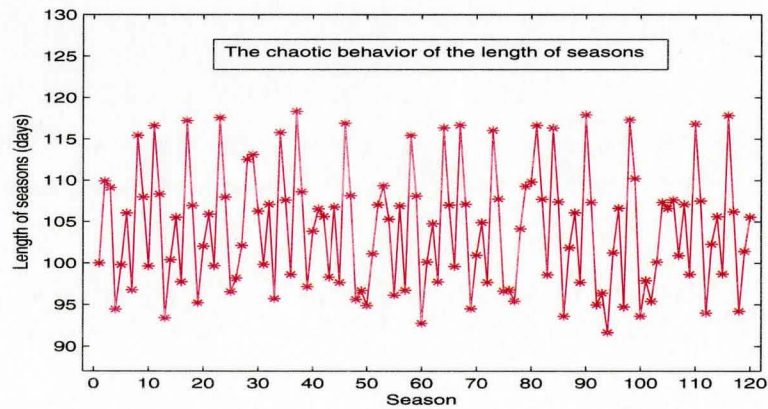


Figure 3.3: The time series of the length of seasons  $L_n$ . The parameters are  $\mathcal{R}_0 = 24$ ,  $N = 6 \times 10^7$ ,  $\Lambda = 0.057$ ,  $K = 12$ ,  $\sigma_1 = 0.01$ ,  $\sigma_K = 0.75$ . When  $\mathcal{R}_0$  is large, the dynamics of  $L_n$  appears chaotic.

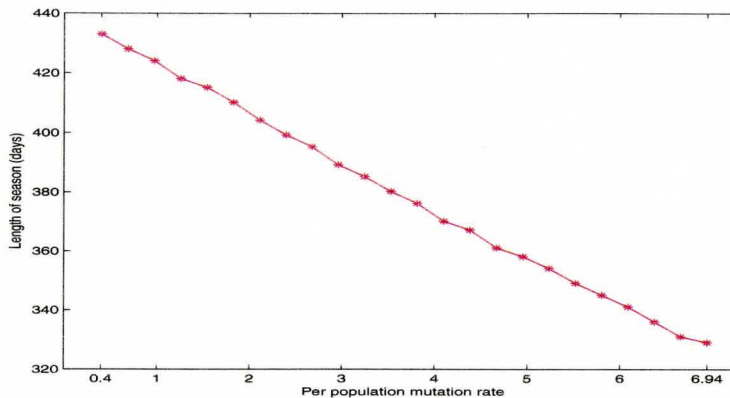


Figure 3.4: The asymptotic trajectory of season length  $L_n$  v.s. the mutation rate ( $\alpha$ ), with  $N = 1.3 \times 10^9$ ,  $\mathcal{R}_0 = 5$ ,  $K = 12$ ,  $\sigma_1 = 0.01$ ,  $\sigma_K = 0.75$ . We can see that the asymptotic season length decreases with the mutation rate  $\alpha$ .

$K = 12$ ,  $\sigma_1 = 0.01$ ,  $\sigma_K = 0.75$ . We can see that  $L_n$  is a decreasing function of  $\alpha$ . This is because the mutation time  $T_{\text{mut}}$  is a decreasing function of  $\alpha$ .

### 3.3 The dependence on the population size $N$

In this section, we try to answer the question of how  $L_n$  depends on the population size  $N$ .  $N$  appears in our model in two places: the initial condition  $I_n(0) = \frac{1}{N}$ ; and the mutation rate  $\alpha = \alpha_{\text{ind}}N$ . If we keep  $\alpha$  constant, then increasing  $N$  decreases  $I_n(0)$ , which increases the length of each epidemic, while keeping the shape of the epidemic curve constant. Thus the mutation time is the same relative to the peak of the epidemic. Hence, increasing  $N$  not only prolongs the epidemic, but delays the mutation time as well. Thus we should expect an increase of  $L_n$ . This is demonstrated in figure 3.5, with parameters  $\alpha = 2.314$ ,  $\mathcal{R}_0 = 5$ ,  $K = 12$ ,  $\sigma_1 = 0.01$ ,  $\sigma_K = 0.75$ .

If we keep the per capita mutation rate  $\alpha_{\text{ind}}$  constant, then the increasing of  $N$  increases  $\alpha$  as well, which, as we know above, increases  $L_n$ . This effect will interfere

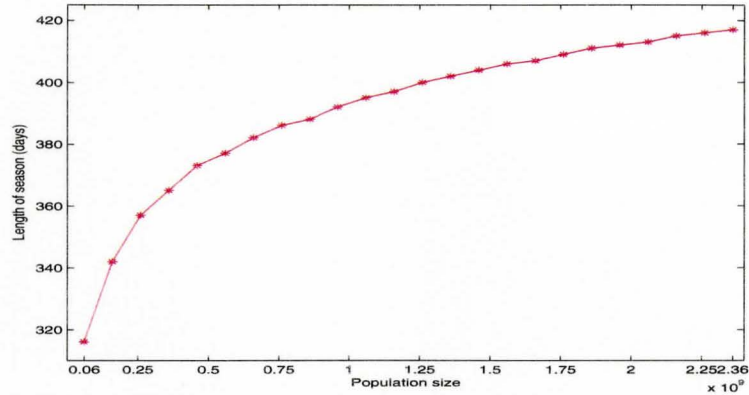


Figure 3.5: The asymptotic trajectory of season length  $L_n$  v.s. the population size while keeping the mutation rate ( $\alpha$ ) constant. The parameters are  $\alpha = 2.314$ ,  $\mathcal{R}_0 = 5$ ,  $K = 12$ ,  $\sigma_1 = 0.01$ ,  $\sigma_K = 0.75$ . The asymptotic season length increases with the population size  $N$  if the mutation rate  $\alpha$  is kept constant.

with the effect of decreasing  $I_n(0)$ . The result is shown in figure 3.6, with parameters  $\alpha_{\text{ind}} = 1.78 \times 10^{-9}$ ,  $\mathcal{R}_0 = 5$ ,  $K = 12$ ,  $\sigma_1 = 0.01$ ,  $\sigma_K = 0.75$ ,

### 3.4 The dependence on the cross-immunity parameters $\sigma_1$ and $\sigma_K$

Here we study the effect of cross-immunity  $1 - \sigma_1$  and  $1 - \sigma_K$  on the length of season  $L_n$ . Figure 3.7 shows that  $L_n$  is an increasing function of the cross immunity  $1 - \sigma_1$  when we keep  $\sigma_K$  constant, with  $\alpha_{\text{ind}} = 1.78 \times 10^{-9}$ ,  $\mathcal{R}_0 = 5$ ,  $N = 6 \times 10^7$ ,  $K = 12$ ,  $\sigma_K = 0.75$ . Figure 3.8 shows that  $L_n$  increases with  $1 - \sigma_K$  as well, with  $\alpha_{\text{ind}} = 1.78 \times 10^{-9}$ ,  $\mathcal{R}_0 = 5$ ,  $N = 6 \times 10^7$ ,  $K = 12$ ,  $\sigma_1 = 0.01$ .

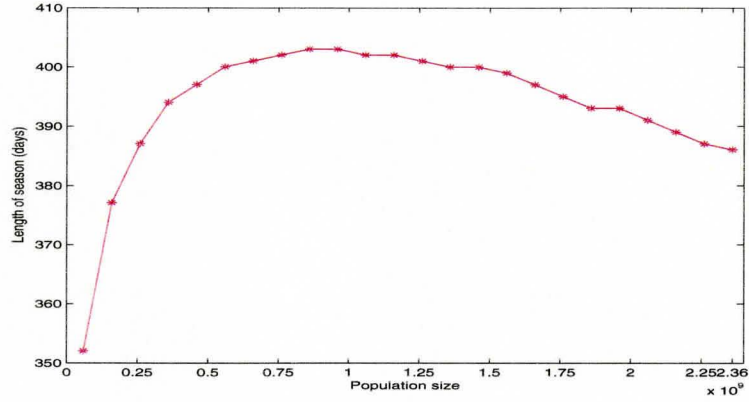


Figure 3.6: The asymptotic trajectory of season length  $L_n$  v.s. the population size while keeping the per capita mutation rate ( $\alpha_{\text{ind}}$ ) constant. The parameters are  $\alpha_{\text{ind}} = 1.78 \times 10^{-9}$ ,  $\mathcal{R}_0 = 5$ ,  $K = 12$ ,  $\sigma_1 = 0.01$ ,  $\sigma_K = 0.75$ . The population size  $N$  affects both the mutation rate  $\alpha$  and the initial condition  $I(0)$  if we keep  $\alpha_{\text{ind}}$  constant. When  $N$  is small, the effect of  $I(0)$  dominates; when  $N$  is large, the effect of  $\alpha$  dominates.

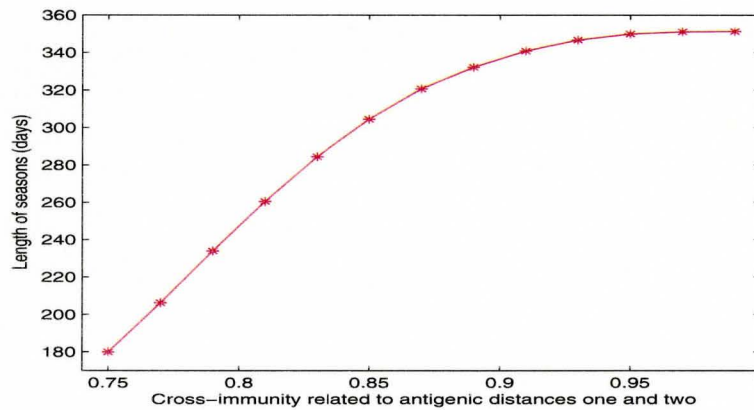


Figure 3.7: The asymptotic trajectory of season length  $L_n$  v.s. the cross-immunity parameter ( $1 - \sigma_1$ ) while keeping  $\sigma_K$  constant. The parameters are  $\alpha_{\text{ind}} = 1.78 \times 10^{-9}$ ,  $\mathcal{R}_0 = 5$ ,  $N = 6 \times 10^7$ ,  $K = 12$ ,  $\sigma_K = 0.75$ . This shows that the asymptotic season length increases with  $1 - \sigma_1$ .

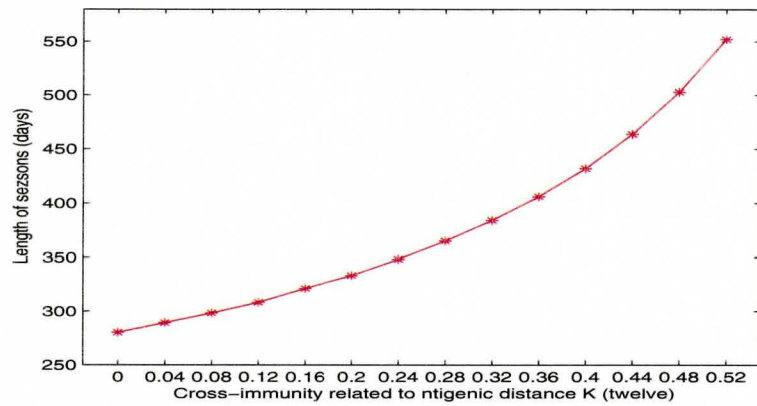


Figure 3.8: The asymptotic trajectory of season length  $L_n$  v.s. the cross-immunity parameter  $(1 - \sigma_K)$  while keeping  $\sigma_1$  constant. The parameters are  $\alpha_{\text{ind}} = 1.78 \times 10^{-9}$ ,  $\mathcal{R}_0 = 5$ ,  $N = 6 \times 10^7$ ,  $K = 12$ ,  $\sigma_1 = 0.01$ . This shows that the asymptotic season length increases with  $1 - \sigma_K$ .

# Chapter 4

## Comparison to the model of Andreasen [2003]

### 4.1 Reducing the competition model Eqs. (2.10) to the model of Andreasen [2003]

If we ignore the transmission from  $I_{n+1}$  to  $S_i$  for  $i < n$ , then the transmission model (2.10) becomes

$$\dot{S}_i = -\beta S_i \sigma_{n-i} (I_n + I_{n+1,n}), \quad i < n, \quad (4.1a)$$

$$\dot{I}_n = \beta \sum_{i=1}^{n-1} \sigma_{n-i} S_i (I_n + I_{n+1,n}) - \gamma I_n, \quad (4.1b)$$

$$\dot{S}_n = -\beta \sigma_1 S_n (I_{n+1} + I_{n,n+1}) + \gamma I_n, \quad (4.1c)$$

$$\dot{I}_{n,n+1} = \beta \sigma_1 S_n I_{n,n+1} - \gamma I_{n,n+1}, \quad (4.1d)$$

$$\dot{S}_{n+1} = \gamma I_{n,n+1}. \quad (4.1e)$$



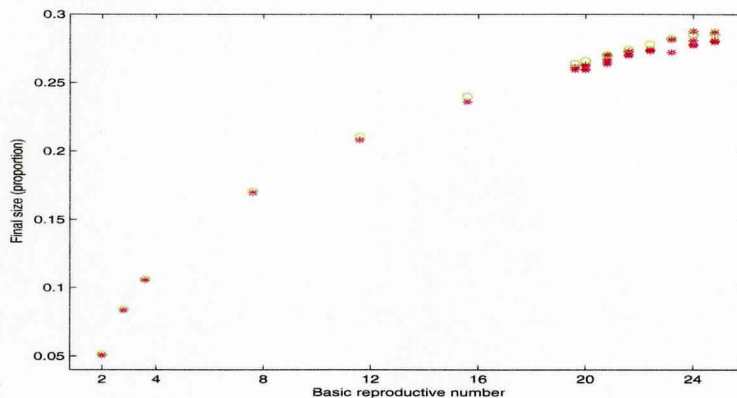


Figure 4.2: The final size  $Z_n$  v.s.  $\mathcal{R}_0$ . The parameters are  $\Lambda = 5.7$ ,  $N = 6 \times 10^7$ ,  $K = 12$ ,  $\sigma_1 = 0.01$ ,  $\sigma_K = 0.75$ . The trajectories of our model are presented by stars, while the trajectories of the model of Andreasen [2003] are presented by circles. The dynamics of  $Z_n$  of the two models diverge when  $\mathcal{R}_0$  becomes large.

produce almost identical final size, but they become more different as  $\mathcal{R}_0$  gets bigger. When  $\mathcal{R}_0 \gg 1$ , our model becomes chaotic, while the model of Andreasen [2003] still converges to a stable equilibrium.

A similar result is shown in figure 4.3. The dynamics of the final size of the two models diverge when the cross-immunity  $1 - \sigma_1$  becomes small.

Figure 4.4 shows the time series of the final size  $Z_n$  with 120 random initial conditions (with parameters  $\alpha_{\text{ind}} = 1.78 \times 10^{-9}$ ,  $\mathcal{R}_0 = 5$ ,  $N = 6 \times 10^7$ ,  $K = 12$ ,  $\sigma_1 = 0.01$ ,  $\sigma_K = 0.75$ ). It shows that the basins of attraction of the two models are different: among the trajectories starting from 120 random initial conditions, one converges to a two-cycle instead of an asymptotically stable equilibrium.

Hence, our model cannot always be reduced to the model of Andreasen [2003]. In some regions of the parameter space, the difference in the variant introduction time and the competition of the mutants and their parents change the dynamics.

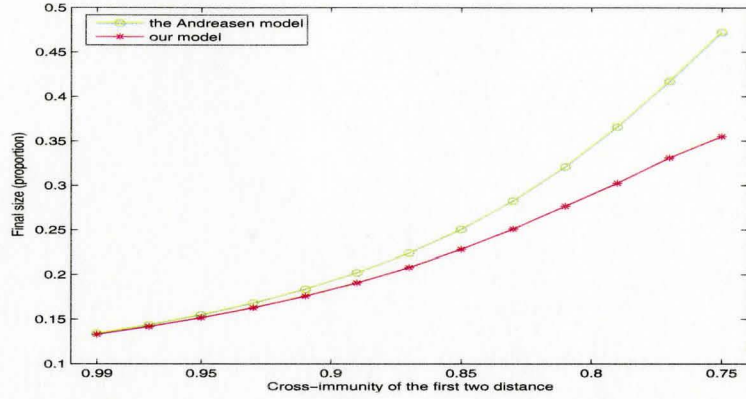
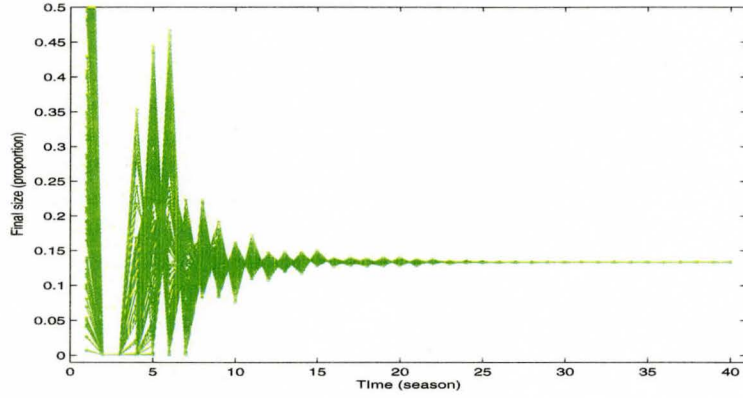


Figure 4.3: The final size  $Z_n$  v.s.  $1 - \sigma_1$ . The parameters are  $\Lambda = 5.7$ ,  $N = 6 \times 10^7$ ,  $\mathcal{R}_0 = 5$ ,  $K = 12$ ,  $\sigma_K = 0.75$ . The trajectories of our model are presented by stars, while the trajectories of the model of Andraesen [2003] are presented by circles. The dynamics of  $Z_n$  of the two models diverge when  $1 - \sigma_1$  becomes small.

a)



b)

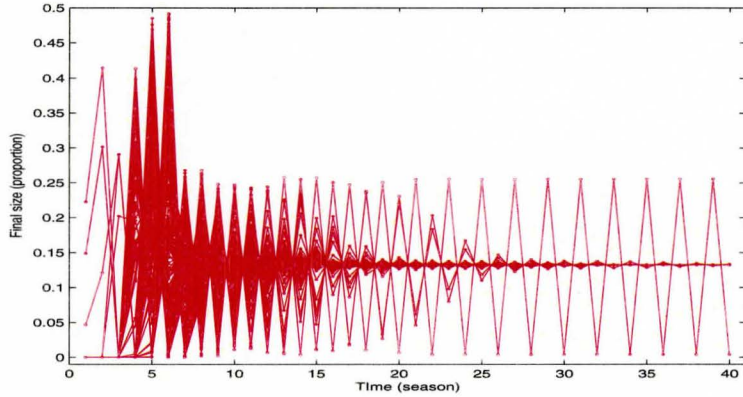


Figure 4.4: a) The time series of the final size  $Z_n$  of the model of Andreasen [2003]), starting with 120 random initial conditions. b) The time series of the final size  $Z_n$  of our model, starting with the same 120 initial conditions as in panel a. The parameters are  $\alpha_{ind} = 1.78 \times 10^{-9}$ ,  $\mathcal{R}_0 = 5$ ,  $N = 6 \times 10^7$ ,  $K = 12$ ,  $\sigma_1 = 0.01$ ,  $\sigma_K = 0.75$ . This shows that the basins of attraction of the two models are different: among the trajectories starting from 120 random initial conditions, one converges to a two-cycle instead of an asymptotically stable equilibrium.

# Chapter 5

## Regulating the length of seasons

Although our model can produce sustained stable cyclic epidemics, the length of season  $L_n$  is a function of the parameters. In general,  $L_n$  does not converge to a year as we observed in death time series. Dushoff et al. [2004] suggest that small-amplitude seasonally forced transmission rates can couple with the intrinsic damped oscillation of the standard SIRS model and regulate the oscillation to a period close to a year. On the other hand, large-amplitude seasonal forcing tends to generate chaotic dynamics in the SIR model with birth/deaths [Olsen and Schaffer, 1990, Kamo and Sasaki, 2002]. In this section, we study how seasonally forcing the transmission rate affects the length of season generated by our model.

We use a sinusoidal seasonal forcing, *i.e.*, the transmission rate is

$$\beta(t) = \bar{\beta} \left[ 1 + A \cos \frac{2\pi t}{365} \right].$$

We try to locate the regions of the parameter space where small seasonal forcing ( $0 < A < 0.026$ ) can regulate the long-term average of the season length to one year. To do so, we fix the population size  $N$ , the mutation rate  $\alpha$  and the

cross-immunity parameters  $(1-\sigma_1)$  and  $(1-\sigma_K)$ , so that the asymptotic season length (denoted as  $L_\infty(A=0)$ ) of the unforced model depends only on the basic reproduction number  $\mathcal{R}_0$ . We then vary  $\mathcal{R}_0$  (and consequently vary  $L_\infty(0)$ ) and  $A$ , and compute the average of  $L_n(A)$ .

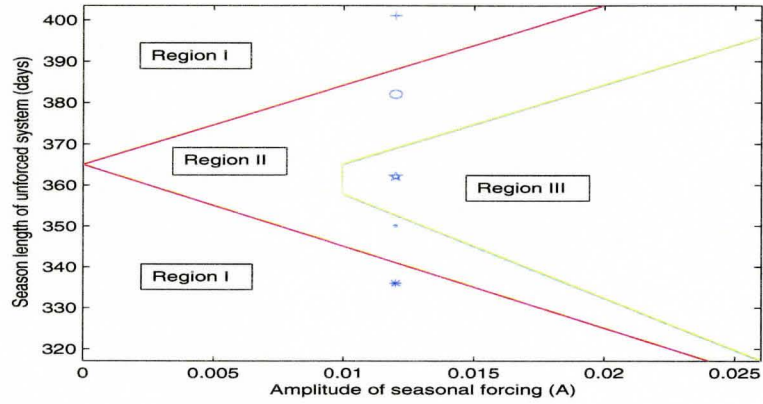
The results are shown in figure 5.1. In region I,  $L_n(A)$  does not converge to an equilibrium, and the mean season length  $\bar{L}(A)$  is not a year. In region II,  $L_n(A)$  converges to a year asymptotically. In region III  $L_n(A)$  converges to a periodic orbit, and the average season length  $\bar{L}(A) = \frac{1}{n} \sum_{i=1}^n L_n(A)$  equals one year.

If we fix  $\mathcal{R}_0$  and vary  $N$  instead, the resulting regions are identical to the regions we find by fixing  $N$  and varying  $\mathcal{R}_0$ . This suggests that no matter what parameter combinations we use to compute the season length of the unforced model  $L_n(A=0)$ , the regions shown in figure 5.1 will not change.

Hence, in our model, small-amplitude seasonal forcing can regulate the season length as well, if the season length of the unforced model is close to one year. This effect only depends on the season length of the unforced model. This conclusion is similar to that of Dushoff et al. [2004].

Interestingly, as seen in the bottom panel of figure 5.1, if the season length of the unforced system  $L_n(0)$  is far from one year, then the seasonally forced system shows chaotic behavior even if  $A$  is small.

a)



b)

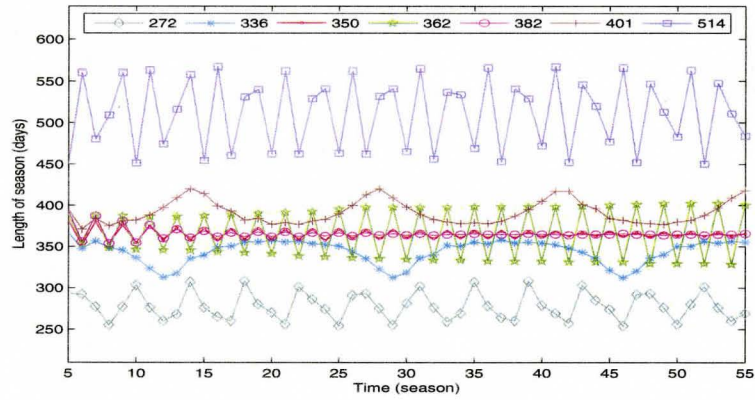


Figure 5.1: a) Regions in the parameter space that yield qualitatively different behavior of the asymptotic season length  $L_\infty$ . In regions II and III the average season length is one year. b) The time series of  $L_n$  in each region (with  $A = 0.012$ ). The parameters are  $\alpha_{ind} = 1.78 \times 10^{-9}$ ,  $N = 6 \times 10^7$ ,  $K = 12$ ,  $\sigma_1 = 0.01$ ,  $\sigma_K = 0.75$ . It shows that small seasonal forcing can regulate the average season length to one year, if the period of the unforced system is close to one year. If the period of the unforced system is very different from one year, the seasonally forced system shows chaotic dynamics.

# Chapter 6

## Conclusions and discussions

In this report, we developed a model that combines a stochastic mutation process with a two-strain competition process. We showed that for a reasonably sized closed population, the mutation process produces a linear phylogeny of the mutant strains. It also justifies the cross-immunity function used in the model of Andreasen [2003].

Our deterministic model, where we use the expected mutation time as the mutation time, can generate sustained stable cyclic epidemics. We can naturally define seasons and compute the length of seasons numerically. With a reasonable basic reproduction number  $\mathcal{R}_0$  and per population mutation rate  $\alpha$ , the length of season converges to an equilibrium value, which is generally a function of the basic reproduction number  $\mathcal{R}_0$ , the per population mutation rate  $\alpha$ , the population size  $N$ , and the cross-immunity parameters. Our stochastic model, where the mutation time are generated randomly, yields stochastic perturbations to the solutions of the deterministic model.

If we ignore the competition between the mutants and their parents, our model is identical to the less realistic model of Andreasen [2003]. Even when we include competition, for a large range of parameter values, our model and the Andreasen model

produce almost identical attractors of the final size in each season. However, the attractors of these two models do not have identical basins of attraction. In the example we emphasized, the model of Andreasen [2003] has a unique attractor, whereas our model has two, including a biennial cycle with basin of attraction comprising around 1% of the initial conditions.

Small-amplitude seasonally forced transmission rates can regulate the season length to an average of one year if the season length of the unforced model  $L_n(A = 0)$  is not far from one year. This is similar to the result of Dushoff et al. [2004]. However, when  $L_n(A = 0)$  is far from one year, the dynamics of the season length may be chaotic, even if the seasonal force is small.

The extent to which stochasticity of the mutation process will destabilize the attractors of the season length is an interesting open question.

Our model ignores migration, which is critical to the results. With migration, the phylogeny would not be linear. This will greatly affect the two-strain competition model. Very large mutation rates invalidate the linear phylogeny as well, because a strain will produce multiple coexisting mutants in a season.

To generalize this model to cases other than linear phylogeny will be a valuable improvement. The improved model could then be coupled to a patch model. Such a patch model may provide useful insights into how spatial heterogeneity affects the evolution of influenza.

# Bibliography

- Roy M. Anderson and Robert M. May. *Infectious Diseases of Humans: Dynamics and Control*. Oxford University Press, Oxford, 1991.
- V. Andreasen, J. Lin, and S. A. Levin. The dynamics of cocirculating influenza strains conferring partial cross-immunity. *Journal of Mathematical Biology*, 35: 825–842, 1997.
- Viggo Andreasen. Dynamics of annual influenza epidemics with immuno-selection. *J. Math. Bio.*, 46(6):504–536, 2003.
- N. T. J. Bailey. *The mathematical theory of infectious diseases and its application*. Griffin, London, second edition, 1975.
- R. M. Bush, C. A. Bender, K. Subbarao, N. J. Cox, and W. M. Fitch. Predicting the evolution of human influenza A. *Science*, 286(5446):1921–1925, 1999.
- Centers for Disease Control and Prevention. Key facts about influenza and the influenza vaccine. Technical report, Centers for Disease Control and Prevention, July 2005. <http://www.cdc.gov/flu/keyfacts.htm>.
- J.H.P. Dawes and J.R. Gog. The onset of oscillatory dynamics in models of multiple diseases strains. *Jour. Math. Biol.*, 45:471–510, 2002.

- O. Diekmann and J. A. P. Heesterbeek. *Mathematical epidemiology of infectious diseases: model building, analysis and interpretation*. Wiley Series in Mathematical and Computational Biology. John Wiley & Sons, LTD, New York, 2000.
- Jr. Douglas, R.G. *The influenza viruses and influenza*. Academic, New York, 1975.
- J. Dushoff, J. B. Plotkin, S. A. Levin, and D. J. D. Earn. Dynamical resonance can account for seasonality of influenza epidemics. *Proceedings of the National Academy of Sciences of the United States of America*, 101:16915–16916, 2004.
- D. J. D. Earn, J. Dushoff, and S. A. Levin. Ecology and evolution of the flu. *Trends in Ecology and Evolution*, 17(7):334–340, 2002.
- D. J.D. Earn, J. Ma, C. T. Bauch, A. P. Galvani, J. B. Plotkin, and J. Dushoff. The persistence of influenza after a pandemic. *Nature*, submitted.
- N. M. Ferguson, A. P. Galvani, and R. M. Bush. Ecological and immunological determinants of influenza evolution. *Nature*, 422(6930):428–433, 2003.
- P. Fine. *Influenza models: peospects for development and use*. MTP press, Lancaster, 1982.
- B. F. Finkenstadt, A. Morton, and D. A. Rand. Modelling antigenic drift in weekly flu incidence. *preprint*, 2004.
- W. M. Fitch, R. M. Bush, C. A. Bender, and N. J. Cox. Long term trends in the evolution of H(3) HA1 human influenza type A. *Proceedings of the National Academy of Sciences of the United States of America*, 94(15):7712–7718, 1997.
- Health Canada. The flu. Technical report, Health Canada, October 2003. <http://www.hc-sc.gc.ca/english/iyh/diseases/flu.html>.

- E. C. Holmes. 1918 and all that. *science*, 303:1787–1788, 2004.
- N. P. Johnson and J. Mueller. Updating the accounts: Global mortality of the 1918 spanish influenza pandemic. *Bull. Hist. Med.*, 76:105–115, 2002.
- M. Kamo and A. Sasaki. The effect of cross-immunity and seasonal forcing in a multi-strain epidemics model. *Phys. D*, 165:228–241, 2002.
- E. D. Kilbourne. *Influenza*. Plenum Medical Books, New York, USA, 1987.
- Juan Lin, Viggo Andreasen, and Simon A. Levin. Dynamics of influenza A drift: the linear three-strain model. *Mathematical Biosciences*, 162:33–51, 1999.
- J. Ma and D. J.D. Earn. Generality of the final size formula for an epidemic of a newly invading infectious disease. *Bulletin for Mathematical Biology*, to appear.
- A. S. Monto. Epidemiology of viral respiratory infections. *Am. J. Med.*, 112:45–125, 2003.
- Karl G. Nicholson, Robert G. Webster, and Alan J. Hay, editors. *Textbook of influenza*. Blackwell Science, London, 1998.
- L. F. Olsen and W. M. Schaffer. Chaos versus noisy periodicity: alternative hypotheses for childhood epidemics. *Science*, 249:499–504, 1990.
- C. M. Pease. An evolutionary epidemiologic mechanism, with applications to type-a influenza. *Theoretical Population Biology*, 31(3):422–452, 1987.
- J. B. Plotkin and J. Dushoff. Codon bias and frequency-dependent selection on the hemagglutinin epitopes of influenza a. *Proceedings of the National Academy of Sciences*, 100:7152–7157, 2003.

- A. H. Reid and J. K. Taubenberger. The origin of the 1918 pandemic influenza virus: a continuing enigma. *J. Gen. Virol.*, 84:2285–2292, 2003.
- J.L. Schulman and E.D. Kilbourne. Airborne transmission of influenza virus infection in mice. *Nature*, 195:1129–1130, 1962.
- L. Simonsen, M. J. Clarke, L. B. Schonberger, N. H. Arden, N. J. Cox, and K. Fukuda. Pandemic versus epidemic influenza mortality: A pattern of changing age distribution. *Journal of Infectious Diseases*, 178(1):53–60, 1998.
- R. G. Webster, W. J. Bean, O. T. Gorman, T. M. Chambers, and Y. Kawaoka. Evolution and ecology of influenza-A viruses. *Microbiological Reviews*, 56(1):152–179, 1992.

# List of Figures

|     |  |    |
|-----|--|----|
| 1.1 | Monthly pneumonia and influenza (P&I) deaths from 1910 to 1998 in the United States. Copyright (2002), TRENDS in Ecology and Evolution [Earn et al., 2002]. The flu seasonality is a striking characteristic.                            | 2  |
| 1.2 | The phylogenic tree of $H_3N_2$ subtype of flu A in $HA_1$ domain. Copyright (1997), National Academic of Science [Fitch et al., 1997]. Subtype $H_3N_2$ mutates quickly. . . . .  | 3  |
| 2.1 | Contour plot of the relative mean first mutation time $\frac{T_{mut}}{T_p}$ vs. the population size $N$ and the basic reproduction number $\mathcal{R}_0$ . The first mutation occurs on average around the peak of an epidemic. . . . . | 16 |
| 2.2 | Contour plot of $\frac{T'_{mut}}{T_p}$ vs. the population size $N$ and the basic reproduction number $\mathcal{R}_0$ , given that the first mutation occurs. We can see that the second mutation occurs late in the epidemic. . . . .    | 17 |

|     |  |    |
|-----|--|----|
| 2.3 | The flow chart of the two-strain competition model (Eqs. (2.10)), where $S_i$ , $i \leq n$ are the proportions of individuals who have been infected by $v_i$ but not $v_k$ for $k > i$ ; $I_n$ and $I_{n+1}$ are the proportion of individuals who come from $S_i$ for $i < n$ and is infectious with $v_n$ and $v_{n+1}$ , respectively; $S_{n+1}$ are the proportion of individuals who have been infected by $v_{n+1}$ but not $v_n$ ; $I_{n,n+1}$ and $I_{n+1,n}$ are the proportion of individuals who come from $S_n$ and $S_{n+1}$ , respectively, and are infectious with $v_{n+1}$ and $v_n$ , respectively; $S_{n,n+1}$ are the proportion of individuals who has been infected sequentially by $v_n$ and $v_{n+1}$ in the same season. | 21 |
| 2.4 | The maximum cross-immunity $1 - \sigma_1$ for the invasion of the variant $v_3$ vs. the reproduction number $\mathcal{R}_0$ . Thus the cross-immunity $1 - \sigma_1$ has to be very small in order for the disease to persist in a totally susceptible population.   | 25 |
| 2.5 | a) The epidemic curve $I(t) = \sum_{i=1}^{\infty} I_i(t) + I_{i+1,i}(t) + I_{i+1}(t) + I_{i,i+1}(t)$ of our deterministic model with parameters $K = 12$ , $\sigma_1 = 0.01$ , $\sigma_K = 0.75$ , $\mathcal{R}_0 = 5$ , $N = 6 \times 10^6$ , $\alpha_{\text{ind}} = 1.78 \times 10^{-9}$ . b) The epidemic curve $I(t)$ of our stochastic model where the mutation time is generated randomly. This shows that our model can indeed produce stable periodic dynamics.  | 27 |
| 3.1 | The definition of the start time of a new season $T_{\text{start}}^n$ .  | 29 |
| 3.2 | The asymptotic trajectory of season length $L_n$ v.s. $\mathcal{R}_0$ . This shows that the asymptotic season length generally decreases with the basic reproduction number $\mathcal{R}_0$ . There is a bifurcation when $\mathcal{R}_0 \approx 19$ . The parameters are $N = 6 \times 10^7$ , $\Lambda = 0.057$ , $K = 12$ , $\sigma_1 = 0.01$ , $\sigma_K = 0.75$ .   | 30 |

|     |  |    |
|-----|--|----|
| 3.3 | The time series of the length of seasons $L_n$ . The parameters are $\mathcal{R}_0 = 24$ , $N = 6 \times 10^7$ , $\Lambda = 0.057$ , $K = 12$ , $\sigma_1 = 0.01$ , $\sigma_K = 0.75$ . When $\mathcal{R}_0$ is large, the dynamics of $L_n$ appears chaotic. . . . .  | 30 |
| 3.4 | The asymptotic trajectory of season length $L_n$ v.s. the mutation rate ( $\alpha$ ), with $N = 1.3 \times 10^9$ , $\mathcal{R}_0 = 5$ , $K = 12$ , $\sigma_1 = 0.01$ , $\sigma_K = 0.75$ . We can see that the asymptotic season length decreases with the mutation rate $\alpha$ . . . . .   | 31 |
| 3.5 | The asymptotic trajectory of season length $L_n$ v.s. the population size while keeping the mutation rate ( $\alpha$ ) constant. The parameters are $\alpha = 2.314$ , $\mathcal{R}_0 = 5$ , $K = 12$ , $\sigma_1 = 0.01$ , $\sigma_K = 0.75$ . The asymptotic season length increases with the population size $N$ if the mutation rate $\alpha$ is kept constant. . . . .  | 32 |
| 3.6 | The asymptotic trajectory of season length $L_n$ v.s. the population size while keeping the per capita mutation rate ( $\alpha_{\text{ind}}$ ) constant. The parameters are $\alpha_{\text{ind}} = 1.78 \times 10^{-9}$ , $\mathcal{R}_0 = 5$ , $K = 12$ , $\sigma_1 = 0.01$ , $\sigma_K = 0.75$ . The population size $N$ affects both the mutation rate $\alpha$ and the initial condition $I(0)$ if we keep $\alpha_{\text{ind}}$ constant. When $N$ is small, the effect of $I(0)$ dominates; when $N$ is large, the effect of $\alpha$ dominates. . . . . | 33 |
| 3.7 | The asymptotic trajectory of season length $L_n$ v.s. the cross-immunity parameter ( $1 - \sigma_1$ ) while keeping $\sigma_K$ constant. The parameters are $\alpha_{\text{ind}} = 1.78 \times 10^{-9}$ , $\mathcal{R}_0 = 5$ , $N = 6 \times 10^7$ , $K = 12$ , $\sigma_K = 0.75$ . This shows that the asymptotic season length increases with $1 - \sigma_1$ . . . . .  | 33 |

|     |  |    |
|-----|--|----|
| 3.8 | The asymptotic trajectory of season length $L_n$ v.s. the cross-immunity parameter $(1 - \sigma_K)$ while keeping $\sigma_1$ constant. The parameters are $\alpha_{\text{ind}} = 1.78 \times 10^{-9}$ , $\mathcal{R}_0 = 5$ , $N = 6 \times 10^7$ , $K = 12$ , $\sigma_1 = 0.01$ . This shows that the asymptotic season length increases with $1 - \sigma_K$ . . . .  | 34 |
| 4.1 | The distribution of the susceptible classes $S_i$ at the start time of a new season: $\mathcal{R}_0 = 4, 7, 10$ and $13$ . The parameters are $\alpha_{\text{ind}} = 1.78 \times 10^{-9}$ , $N = 6 \times 10^7$ , $K = 12$ , $\sigma_1 = 0.01$ , $\sigma_K = 0.75$ . The trajectories of our model are presented by points, while the trajectories of the model of Andreasen [2003] are presented by circles. The two models produce almost identical infection history distributions. . . . . | 36 |
| 4.2 | The final size $Z_n$ v.s. $\mathcal{R}_0$ . The parameters are $\Lambda = 5.7$ , $N = 6 \times 10^7$ , $K = 12$ , $\sigma_1 = 0.01$ , $\sigma_K = 0.75$ . The trajectories of our model are presented by stars, while the trajectories of the model of Andreasen [2003] are presented by circles. The dynamics of $Z_n$ of the two models diverge when $\mathcal{R}_0$ becomes large. . . . .  | 37 |
| 4.3 | The final size $Z_n$ v.s. $1 - \sigma_1$ . The parameters are $\Lambda = 5.7$ , $N = 6 \times 10^7$ , $\mathcal{R}_0 = 5$ , $K = 12$ , $\sigma_K = 0.75$ . The trajectories of our model are presented by stars, while the trajectories of the model of Andreasen [2003] are presented by circles. The dynamics of $Z_n$ of the two models diverge when $1 - \sigma_1$ becomes small. . . . .  | 38 |

4.4 a) The time series of the final size  $Z_n$  of the model of Andreasen [2003]), starting with 120 random initial conditions. b) The time series of the final size  $Z_n$  of our model, starting with the same 120 initial conditions as in panel a. The parameters are  $\alpha_{ind} = 1.78 \times 10^{-9}$ ,  $\mathcal{R}_0 = 5$ ,  $N = 6 \times 10^7$ ,  $K = 12$ ,  $\sigma_1 = 0.01$ ,  $\sigma_K = 0.75$ . This shows that the basins of attraction of the two models are different: among the trajectories starting from 120 random initial conditions, one converges to a two-cycle instead of an asymptotically stable equilibrium. . . . . 39

5.1 a) Regions in the parameter space that yield qualitatively different behavior of the asymptotic season length  $L_\infty$ . In regions II and III the average season length is one year. b) The time series of  $L_n$  in each region (with  $A = 0.012$ ). The parameters are  $\alpha_{ind} = 1.78 \times 10^{-9}$ ,  $N = 6 \times 10^7$ ,  $K = 12$ ,  $\sigma_1 = 0.01$ ,  $\sigma_K = 0.75$ . It shows that small seasonal forcing can regulate the average season length to one year, if the period of the unforced system is close to one year. If the period of the unforced system is very different from one year, the seasonally forced system shows chaotic dynamics. . . . . 42